First record of disk-footed bat *Eudiscopus denticulus* (Chiroptera, Vespertilionidae) from China and resolution of phylogenetic position of the genus

DEAR EDITOR,

The disk-footed bat *Eudiscopus denticulus* (Osgood, 1932) is a rare species in Southeast Asia. During two chiropteran surveys in the summer of 1981 and 2019, eight and three small *Myotis*- like bats with distinct disk-like hindfeet were collected from Yunnan Province, China, respectively. External, craniodental, and phylogenetic evidence confirmed these specimens as *E. denticulus*, representing a new genus in China. The complete mitochondrial genome consistently showed robust support for *E. denticulus* as a basal lineage within Myotinae. The coding patterns and characteristics of its mitochondrial genome were similar to that of other published genomes from *Myotis*. The echolocation signals of the newly collected individuals were analyzed. The potential distribution range of *Eudiscopus* in Southeast Asia inferred using the MaxEnt model indicated its potential occurrence along the southern border region of Yunnan, China.

In 1932, Osgood described a new genus and species of vespertilionid bat based on six specimens collected at Phong Saly in northern Laos, externally resembling a small *Myotis* species but with a striking adhesive disk on the hindfoot and with a flattened skull, and was named *Discopus denticulus* Osgood, 1932. Conisbee (1953) noted, however, that the name *Discopus* was preoccupied and proposed *Eudiscopus* as a replacement name. Till today, only a limited number of specimens have been found in Southeast Asia and the biological information available on the species is limited (Wilson & Mittermeier, 2019). Presently, the species is reported from Laos (Osgood, 1932), Myanmar (Koopman, 1970), Thailand (Kock & Kovac, 2000; Soisook et al., 2016), and Vietnam (Kruskop, 2010, 2013; Zsebők et al., 2014) (Figure 1F). Based on morphological examinations and phylogenetic analyses of 11 specimens collected from Yunnan, we herein report on the first occurrence of this poorly known bat from China.

Due to the limitation of available samples and sequences of *E. denticulus*, its phylogenetic position remains contradictory. Traditional morphology-based systematics place it within Vespertilioninae (Simmons, 2005; Tate, 1942), or close to *Myotis* (Borisenko & Kruskop, 2003). Several phylogenies support the inclusion of *E. denticulus* in Myotinae (Amador et al., 2018; Tsytsulina et al., 2007; Yu et al., 2014); whereas others reveal different positions, including placement outside of Myotinae (Amador et al., 2018; Shi & Rabosky, 2015), or — albeit with low support — as a sister taxon to *Hesperoptenus tickelli* (Görföl et al., 2019). Clarifying its phylogenetic position would not only improve our understanding of the morphological evolutionary process of this unique species but also help determine the convergent evolution of flattened skulls and the presence of the disk-like hindfoot in Vespertilionidae. Two data matrices representing a large-scale

Received: 07 August 2020; Accepted: 15 December 2020; Online: 18 December 2020

Foundation items: This study was financially supported by the National Natural Science Foundation of China (31970394, 31670381, 31672258), Guangzhou University's 2017 Training Program for Young High-Achieving Personnel (BJ201707), Science-Technology Basic Condition Platform from the Ministry of Science and Technology of the People's Republic of China (2005DKA21402), Lancang-Mekong Cooperation Special Fund (Biodiversity Monitoring and Network Construction Along Lancang-Mekong River Basin Project), and Biodiversity Investigation in Xishuangbanna National Nature Reserve, Biodiversity Investigation, Observation, and Assessment Program (2019-2023) of the Ministry of Ecology and Environment of China (8-2-3-4-5), Scientific Research Foundation of the Education Department of Sichuan Province, China (11ZA164), and Research Foundation of Mianyang Teachers' College (MYHQ2016A01). Gabor Csorba received support from the National Research, Development, and Innovation Fund of Hungary (NKFIH KH130360) and SYNTHESYS Project, which is financed by the European Community Research Infrastructure Action under the FP7 "Capacities" Program

DOI: 10.24272/j.issn.2095-8137.2020.224

sampling of Vespertilionidae (~5 kb, 360 species) and a compilation of all currently deposited complete mitochondrial genomes (~15 kb, 101 species) were herein generated to determine the phylogenetic position of this species. Acoustic characteristics of the echolocation calls were further analyzed. Through maximum entropy (MaxEnt) modelling, potentially suitable habitats were also inferred.

Eudiscopus denticulus from China was sampled from three sites in Xishuangbanna, Yunnan Province (see Supplementary Data). The eight specimens sampled in 1981 were initially misidentified as *Tylonycteris* sp. but were reclassified as *E. denticulus* in 2019. All specimens in the study are adults based on the status of the epiphyseal cartilage gap in the metacarpal joint (Kunz & Anthony, 1982). They are presently stored in the collections of the Kunming Institute of Zoology, Chinese Academy of Sciences, Yunnan, China (KIZ 811 351–811 358) and the School of Life Sciences, Guangzhou University, Guangdong, China (GZHU 19 159, 19 160, 19 164). The specimens are all small-sized individuals with a forearm length of 34.8–38.5 mm (Table 1), and externally resemble a small

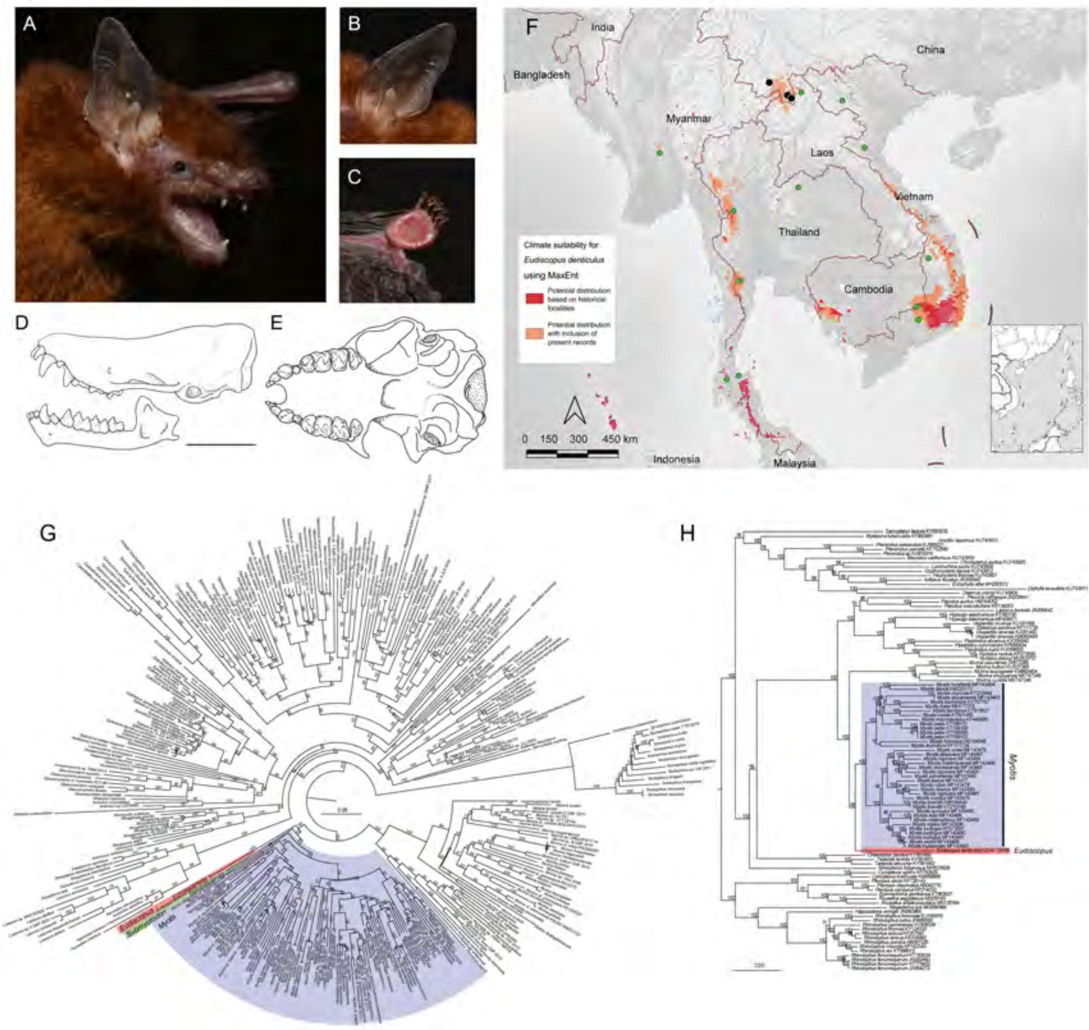

Figure 1 External (A–C), skull, and dentition (D, E) characteristics of *Eudiscopus denticulus* from China (GZHU 19 159), its potential distribution areas in Southeast Asia predicted by MaxEnt (F), and two maximum-likelihood phylogenetic trees using IQ-tree (G, H)

Live individual (A), ear (B), and hindfoot (C); lateral view of skull and mandible (D); ventral view of skull (E). Scale bar: 5 mm. Photos by Yi Wu (A–C); drawings by Wen-Hua Yu (D, E). F: Black circles mark sampling localities in Xishuangbanna, Yunnan, China; green circles represent historical occurrences from literature and Global Biodiversity Information Facility (GBIF) database (Occurrence dataset https://doi.org/10.15468/igaciv accessed via GBIF.org on 2019-10-14). Red regions are good potential distributions based on localities known so far; orange areas are predictions with inclusion of present records. G: Phylogenetic tree containing 360 presumed vespertilionid species representing large-scale sampling strategy. H: Phylogenetic tree based on 101 complete mitochondrial sequences. Red, green, and blue trapezoids represent *Eudiscopus, Submyotodon*, and *Myotis*, respectively.

Myotis species. The fur is dense and soft, reddish brown at the dorsum (Figure 1A). The ears reach the tip of the muzzle when laid forward, and the tragus is straight and distinctly narrowing, ending in a blunt tip (Figure 1B). Noticeable disk-like adhesive pads are present on the feet, similar to that in *Tylonycteris* and *Glischropus* but more pronounced ventrally (Figure 1C). The skull is relatively broad and strikingly flattened; rostrum is elongated and relatively long and upturned anteriorly (Figure 1D, E). Dental formula is I 2/3, C 1/1, P 2/3, M 3/3. Upper canine is *Myotis*- like without any supplementary cusps; first upper incisor is higher than the second, as in *Myotis*, p_3 is largely reduced, displaced to the lingual side of the tooth row, and compressed between p_2 and p_4; lower molars are myotodont (Figure 1D, E). Detailed information and measurements of all specimens used in this study are listed in Table 1 and Supplementary Appendix I. To illustrate potential geographic variation, principal component analysis (PCA) with varimax rotation and *t*- test were performed. According to the integrity of our data, 10 craniodental measurements were selected in the PCA. The first two components (44% and 33% for principal components PC1 and PC2, respectively) accounted for 77% of total variance (Supplementary Figure S1). For PC1, greatest length of skull (GTL), length of maxillary toothrow (UCM^3L), length of mandibular toothrow (LCM_3L), and greatest length of mandible (MANL) had high positive loadings (Table 1), reflecting an external overall size effect. PC2 was mostly related to braincase height (BCH), mastoid width (MAW), and interorbital width (IOW) (Table 1), generally implying width and height of braincase. These patterns indicated that individuals from China and Laos have a wider and more flattened braincase than those from the middle regions of Vietnam and Myanmar (Table 1 and Supplementary Figure S1). Such differences were also revealed from comparisons between China and Vietnam using *t*- test, which additionally revealed a longer forearm in the Chinese population (Table 1).

The complete mitochondrial genome of *E. denticulus* was ~16 500 bp in length, containing 13 protein-coding genes, two ribosomal RNA genes, 22 transfer RNA genes, and a control region (GenBank accession No.: MW085031 for GZHU 19159, Supplementary Figure S2). Most genes were encoded on the H-strand, except for eight *t*RNA and *ND6* genes. The coding patterns and characteristics are similar to those in other published mitochondrial genomes of Myotinae (e.g., Chung et al., 2018; Jebb et al., 2017; Jiang et al., 2016; Platt et al., 2017; Yu et al., 2016). Our large-scale vespertilionid maximum-likelihood phylogenies highly supported *E. denticulus* as a monophyletic clade (bootstrap value: 100; Figure 1G and Supplementary Figures S3A) as well as its inclusion within Myotinae (Figure 1G, H). Furthermore, *E. denticulus* appeared as a sister taxon to a clade clustering *Myotis* and *Submyotodon*, indicating a basal position within Myotinae (Figure 1G). For intraspecific relationships, an ambiguous haplotype network emerged, which implied a close matrilineal relationship between our samples and individuals from Bu Gia Map National Park, BinhPhuc, Vietnam, based on mitochondrial markers (GenBank accession No. of Chinese individuals: MT822523 for GZHU 19159, MT822524 for GZHU 19160; Supplementary Figure S3B).

Eudiscopus denticulus uses a broadband, downward frequency modulated (FM) call when flying in closed environments (see Supplementary Data; Supplementary Figure S4). Both our recordings and those from Zsebők et al. (2014), from specimens flying in a tent or room, showed a broadband FM signal with a narrowband FM end, rather than the broadband FM calls reported by Hughes et al. (2011) in two individuals released in a cluttered environment. The call structure and relatively long and broad wings support the view that *E. denticulus* is an edge space aerial forager (Schnitzler et al., 2003; Zsebők et al., 2014). From the specimens in China, specifically, the maximum start frequency was found to be around 98 kHz, and the minimum end frequency was around 50 kHz (Table 1). At the start of the echolocation call, the narrowband FM portion was always relatively short (Supplementary Figure S4). The maximum energy was at 53.3 kHz, on average (Supplementary Figure S4), while the mean length of the echolocation calls was around 3.1 ms (Table 1). The geographic differences in morphological measurements were mirrored in the acoustic signals, as our samples emitted lower frequency echolocation calls (e.g., highest frequency (HF), lowest frequency (LF), and frequency with most energy (FMAX)) than those from Vietnam (Zsebők et al., 2014) (Table 1). These differences seem to be in line with the negative correlation between body size and call frequency (Barclay et al., 1999; Robinson, 1996; Schnitzler & Kalko, 2001; Yoshino et al., 2006); however, more elaborate experiments are needed to verify these differences due to the variances in methods used for recording, which may have affected echolocation parameters.

As the present record is the northernmost locality of *E. denticulus*, we ran two MaxEnt models (with and without the new record) to evaluate its influence on potential distribution of the species. Both model outputs provided satisfactory results, with AUC values of the models with and without our records of 0.89 and 0.75, respectively. Mean temperature of warmest quarter (BIO10) and precipitation of coldest quarter (BIO19) were the most important influencing factors. The model for current potential distribution of *E. denticulus* in Southeast Asia showed that the most suitable habitat is medium warm and moist forest with bamboo stands. The large potential area with the inclusion of the present Chinese records is approximately twice the size as the prediction based on published occurrences so far (Figure 1F). However, the MaxEnt model almost always provides over-estimates compared to the realized niche of a species, as it only considers niche-based presence data and predicts a species' fundamental niche rather than realized niche (Phillips & Dudík, 2008; Phillips et al., 2004). Nevertheless, the inference obtained should facilitate subsequent targeted investigation on this rare species.

In the IUCN Red List, *E. denticulus* was shifted from Lower Risk/Near Threatened in 1996, to Data Deficient in 2008, and

Table 1 Descriptive statistics of external and craniodental measurements, and echolocation parameters of *Eudiscopus denticulus* from China and nearby countries

Index	Yunnan, China	Pu Huong, Vietnam	*t*-value	Pegu, Myanmar	Laos	PC1	PC2
W (g)	5.2±1.14 (11) (4.0－7.0)	－	－	－	－	－	－
HB (mm)	40.5±2.28 (11) (36.0－45.3)	38.0±2.19 (5) (35.9－40.5)	2.06	－	－	－	－
T (mm)	40.3±2.87 (11) (35.0－45.0)	38.8±2.56 (5) (34.9－41.4)	1.05	－	－	－	－
E (mm)	11.2±1.75 (11) (8.0－13.0)	11.6±0.66 (4) (10.9－12.5)	－0.51	－	－	－	－
HF (mm)	6.0±0.82 (11) (5.4－8.1)	6.7±0.63 (5) (5.8－7.2)	－1.56	－	－	－	－
FA (mm)	36.7±1.10 (11) (34.8－38.5)	34.5±0.88 (5) (33.5－35.6)	3.98*	－	－	－	－
Tib (mm)	17.2±0.54 (11) (16.2－17.9)	16.3±0.64 (5) (15.4－16.9)	2.68*	－	－	－	－
GTL (mm)	14.34±0.34 (8) (13.71－14.79)	14.00±0.22 (10) (13.59－14.32)	2.56*	13.43	14.49	**0.81**	0.54
CCL (mm)	13.28±0.28 (8) (12.83－13.74)	12.79±0.21 (11) (12.47－13.04)	4.43*	12.15	13.16	0.72	0.62
CBL (mm)	14±0.32 (8) (13.35－14.42)	－	－	－	－	－	－
BCW (mm)	6.84±0.14 (8) (6.63－7.01)	6.74±0.1 (11) (6.53－6.87)	1.76	6.36	6.99	0.46	0.56
BCH (mm)	4.53±0.23 (8) (4.16－4.78)	3.76±0.12 (11) (3.54－3.97)	8.86*	3.07	3.54	0.35	**0.72**
ZYW (mm)	9.48±0.29 (4) (9.16－9.82)	9.21±0.15 (6) (8.97－9.43)	－	－	－	－	－
MAW (mm)	7.72±0.19 (8) (7.41－7.92)	7.51±0.16 (11) (7.34－7.81)	2.64*	7.20	7.75	0.49	**0.75**
PL (mm)	6.38±0.11 (8) (6.25－6.6)	－	－	－	－	－	－
IOW (mm)	3.73±0.11 (8) (3.60－3.89)	3.61±0.16 (11) (3.4－3.94)	1.95	3.47	3.71	－0.14	**0.87**
UIM^{3}L (mm)	6.42±0.18 (8) (6.12－6.68)	－	－	－	－	－	－
UCM^{3}L (mm)	5.44±0.11 (8) (5.31－5.58)	5.36±0.11 (10) (5.21－5.49)	1.61	5.20	5.48	**0.88**	0.25
UCCW (mm)	3.77±0.06 (8) (3.71－3.91)	3.70±0.09 (9) (3.60－3.91)	1.60^{NS}	3.59	3.80	0.62	0.53
UM^{3}M^{3}W (mm)	5.86±0.12 (8) (5.62－6.01)	5.81±0.09 (10) (5.74－6.05)	1.24	－	5.88	－	－
LIM$_3$L (mm)	6.80±0.15 (8) (6.56－7.06)	－	－	－	－	－	－
LCM$_3$L (mm)	5.74±0.12 (8) (5.54－5.88)	5.70±0.12 (11) (5.52－5.85)	0.77	5.49	5.68	**0.89**	－0.07
MANL (mm)	10.23±0.18 (8) (9.82－10.42)	10.2±0.15 (11) (9.91－10.46)	0.34	9.74	10.63	**0.80**	0.30
PCH (mm)	3.29±0.11 (8) (3.13－3.40)	3.16±0.11 (11) (3－3.38)	2.63*	3.00, 3.09	3.25	－	－
HF (kHz)	98.3±3.25 (24) (92.0－104.0)	108.9 (3) (106.5－112.9)$^{\#}$	－	－	－	－	－
LF (kHz)	49.9±2.02 (24) (45.0－54.4)	52.0 (51.1－53.9)$^{\#}$	－	－	－	－	－
FMAX (kHz)	53.3±1.29 (24) (50.1－55.0)	61.7 (60.9－63.0)$^{\#}$	－	－	－	－	－
DUR (ms)	3.1±0.24 (24) (2.8－3.7)	2.03 (1.87－2.11)$^{\#}$	－	－	－	－	－

Abbreviations can be found in text and Supplementary Materials and Methods. Values are given as means±*SD* (if *n*>3) and minimum-maximum (min-max). *t*-value is from Students *t*-test between China and Vietnam specimens when measurement distribution fits normality, and * represents *P*<0.05. Using a Pettersson D500X ultrasound detector (Pettersson Elektronik AB), echolocation calls were recorded from three Chinese-sampled bats (collected in 2019) flying in a room (5 m×4 m×3 m). $^{\#}$ indicates secondary means and minimum and maximum values based on mean values of three individuals from Zsebők et al. (2014). Note, scores in first parentheses in echolocation measurements indicate number of calls analyzed in this study; those from Zsebők et al. (2014) represent number of individuals in their study. Indices in bold indicate variables used in principal component analysis, PC1 and PC2 scores in bold indicate variables with greatest loadings in respective component. －: Not available.

Least Concern at present. This classification is based on its wide distribution across Southeast Asia, lack of major threats, and no sign of decline at a rate that would qualify it in a threatened category (Soisook et al., 2016). Nevertheless, its rarity and our poor knowledge on its biology have been highlighted (Kock & Kovac, 2000; Koopman, 1970; Kruskop, 2010, 2013; Tsytsulina et al., 2007; Wilson & Mittermeier, 2019). Furthermore, our distribution predictions using MaxEnt show that suitable habitat areas are extremely fragmentary (Figure 1F). Of note, the large temporal gap in capture/collection of this species in China (38 years) also indicates its rarity and fragility. As such, particular conservation attention should be reinforced in the future.

Additional contribution herein refers to the scanning of a skull of *E. denticulus* (KIZ 811355) using a RexcanDS3 Silver 3D Scanner designed for small objects with a maximum resolution of 0.01 mm (Supplementary Figure S5). The scanned PHY files are deposited as supplementary materials (Suppl. PHY files). Although micro-computed tomography (μCT) scanners would capture more accurate details with better resolution, the considerably smaller size of our files than those produced by a μCT scanner (e.g., ~40 MB vs. ~600 MB in the case of a skull scan), and sufficient accuracy suggest that laser 3D scanners can be used as an alternative for shape analyses and morphological studies (Marcy et al., 2018). We believe that 3D digitization and virtual access platforms could facilitate future species determination and boost international academic cooperation.

SCIENTIFIC FIELD SURVEY PERMISSION INFORMATION

Permission for field surveys in Xishuangbanna, Yunnan Province, China, were granted by the Xishuangbanna Nature Reserve Administration.

SUPPLEMENTARY DATA

Supplementary data of this article can be found online.

COMPETING INTERESTS

The authors declare that they have no competing interests.

AUTHORS' CONTRIBUTIONS

W.H.Y., G.C., Y.W., and S.L. designed the study; Z.L. Y.W., R.C.Q., Q.Y.W., Y.W., and S.L. collected materials for the study; W.H.Y., Y.N.L., G.C., H.Y.S., and Y.W. performed morphometric and phylogenetic analyses; W.H.Y., G.C., Y.W., and S.L. interpreted the results and prepared the manuscript, photographs, and figures for the study. All authors read and approved the final version of the manuscript.

ACKNOWLEDGEMENTS

We are grateful to the anonymous referees for their constructive comments. We also thank Yi-Feng Hu, Yang Yue, and Han-Bo Zhang for their help in field survey and assistance during lab work.

Wen-Hua Yu[1], Gabor Csorba[2], Zheng-Lan-Yi Huang[1], Yan-Nan Li[1], Shuo Liu[3], Rui-Chang Quan[4], Qiao-Yan Wang[5], Hong-Yan Shi[6], Yi Wu[1,*], Song Li[3,*]

[1] *Key Laboratory of Conservation and Application in Biodiversity of South China*, *School of Life Sciences*, *Guangzhou University*, *Guangzhou*, *Guangdong* 510006, *China*

[2] *Department of Zoology*, *Hungarian Natural History Museum*, *Budapest H*-1088, *Hungary*

[3] *Kunming Natural History Museum of Zoology*, *Kunming Institute of Zoology*, *Chinese Academy of Sciences*, *Kunming*, *Yunnan* 650223, *China*

[4] *Center for Integrative Conservation*, *Xishuangbanna Tropical Botanical Garden*, *Chinese Academy of Sciences*, *Mengla*, *Yunnan* 666303, *China*

[5] *Research Institute of Xishuangbanna National Nature Reserve*, *Jinghong*, *Yunnan* 666100, *China*

[6] *Ecological Security and Protection Key Laboratory of Sichuan Province*, *Mianyang Teacher's College*, *Mianyang*, *Sichuan* 621000, *China*

*Corresponding authors, E-mail: wuyizhouq@263.net; lis@mail.kiz.ac.cn

REFERENCES

Amador LI, Arévalo RLM, Almeida FC, Catalano SA, Giannini NP. 2018. Bat systematics in the light of unconstrained analyses of a comprehensive molecular supermatrix. *Journal of Mammalian Evolution*, **25**(1): 37−70.

Barclay RM, Fullard JH, Jacobs DS. 1999. Variation in the echolocation calls of the hoary bat (*Lasiurus cinereus*): influence of body size, habitat structure, and geographic location. *Canadian Journal of Zoology*, **77**(4): 530−534.

Chung CU, Kim SC, Jeon YS, Han SH, Yu JN. 2018. The complete mitochondrial genome of long-tailed whiskered bat, *Myotis frater* (Myotis, Vespertilionidae). *Mitochondrial DNA Part B*, **3**(2): 570−571.

Conisbee LR. 1953. A list of the Names Proposed for Genera and Subgenera of Recent Mammals, from the Publication of T. S. Palmer's Index Generum Mammalium, 1904 to the end of 1951. London: British Museum (Natural History).

Görföl T, Furey NM, Bates PJJ, Csorba G. 2019. The identity of '*Falsistrellus*' *affinis* from Myanmar and Cambodia and new records of *Hypsugo dolichodon* from these countries. *Acta Chiropterologica*, **20**(2): 301−309.

Hughes AC, Satasook C, Bates PJJ, Soisook P, Sritongchuay T, Jones G, et al. 2011. Using echolocation calls to identify Thai bat species: vespertilionidae, emballonuridae, nycteridae and megadermatidae. *Acta Chiropterologica*, **13**(2): 447−455.

Jebb D, Foley NM, Kerth G, Teeling EC. 2017. The complete mitochondrial genome of the Bechstein's bat, *Myotis bechsteinii* (Chiroptera, Vespertilionidae). *Mitochondrial DNA Part B*, **2**(1): 92−94.

Jiang JJ, Wang SQ, Li YJ, Zhang W, Yin AG, Hu M. 2016. The complete mitochondrial genome of insect-eating brandt's bat, *Myotis brandtii* (Myotis, Vespertilionidae). *Mitochondrial DNA Part A*, **27**(2): 1403−1404.

Kock D, Kovac D. 2000. *Eudiscopus denticulus* (Osgood 1932) in Thailand with notes on its roost (Chiroptera: Vespertilionidae). *Zeitschrift für Säugetierkunde*, **65**(2): 121−123.

Koopman K. 1970. A second locality for *Eudiscopus denticulus* (Chiroptera, Vespertilionidae). *Journal of Mammalogy*, **51**(1): 191.

Kruskop SV. 2010. Preliminary data on the bat fauna of Bu Gia Map National Park (Southern Vietnam). *Plecotus*, **13**: 69−74.

Kruskop SV. 2013. Bats of Vietnam: Checklist and an Identification Manual. 2nd ed. Moscow: KMK Scientific Press.

Kunz TH, Anthony ELP. 1982. Age estimation and postnatal development in the Mexican free-tailed bat (*Tadarida brasiliensis mexicana*): birth size,

growth rates, and age estimation. *Journal of Mammalgy*, **76**(3): 123−138.
Marcy AE, Fruciano C, Phillips MJ, Mardon K, Weisbecker V. 2018. Low resolution scans can provide a sufficiently accurate, cost- and time-effective alternative to high resolution scans for 3D shape analyses. *PeerJ*, **6**(5): e5032.
Osgood WH. 1932. Mammals of the kelley-roosevelts and delacour asiatic expeditions. *Field Museum of Natural History, Zoology Series*, **18**(10): 193−339.
Phillips SJ, Dudík M. 2008. Modeling of species distributions with MaxEnt: new extensions and a comprehensive evaluation. *Ecography*, **31**(2): 161−175.
Phillips SJ, Dudík M, Schapire RE. 2004. MaxEnt software for species distribution modeling. *In*: Proceedings of the 21st International Conference on Machine Learning. 655–662.
Platt RN, Faircloth BC, Sullivan KAM, Kieran TJ, Glenn TC, Vandewege MW, et al. 2017. Conflicting evolutionary histories of the mitochondrial and nuclear genomes in new world Myotis Bats. *Systematic Biology*, **67**(2): 236−249.
Robinson MF. 1996. A relationship betwen echolocation calls and noseleaf widths in bats of the genera Rhinolophus and Hipposideros. *Journal of Zoology*, **239**(2): 389−393.
Schnitzler HU, Kalko EKV. 2001. Echolocation by insect-eating bats. *Bioscience*, **51**(7): 557.
Schnitzler HU, Moss CF, Denzinger A. 2003. From spatial orientation to food acquisition in echolocating bats. *Trends in Ecolgy & Evolution*, **18**(8): 386−394.
Shi JJ, Rabosky DL. 2015. Speciation dynamics during the global radiation of extant bats. *Evolution*, **69**(6): 1528−1545.
Soisook P, Csorba G, Bumrungsri S, Francis CM, Bates P, Kingston T. 2016. *Eudiscopus denticulus*. The IUCN Red List of Threatened Species, e.T8168A22028419. https://dx.doi.org/10.2305/IUCN.UK.2016-2.RLTS.T8168A22028419.en.
Simmons NB. 2005. Order Chiroptera. *In*: Wilson DE, Reeder DM. Mammal Species of the World: A Taxonomic and Geographic Reference, 3rd edn. Baltimore: The Johns Hopkins University Press, 2142.
Tate GHH. 1942. Review of the vespertilionine bats: with special attention to genera and species of the Archbold collections. *Bulletin of the American Museum of Natural History*, **80**(7): 221−297.
Tsytsulina K, Kruskop S, Ryuichi M. 2007. Taxonomical position of the genus *Eudiscopus* among vespertilionid bats. *Bat Research News*, **44**: 309.
Wilson DE, Mittermeier RA. 2019. Handbook of the Mammals of the World-Volume 9: Bats. Barcelona: Lynx Edicions.
Yoshino H, Matsumura S, Kinjo K, Tamura H, Ota H, Izawa M. 2006. Geographical variation in echolocation call and body size of the Okinawan least horseshoe bat, *Rhinolophus pumilus* (Mammalia: Rhinolophidae), on Okinawa-jima Island, Ryukyu Archipelago, Japan. *Zoological Science*, **23**(8): 661−667.
Yu DN, Qian KN, Storey KB, Hu YZ, Zhan JY. 2016. The complete mitochondrial genome of *Myotis lucifugus* (Chiroptera: Vespertilionidae). *Mitochondrial DNA Part A*, **27**(4): 2423−2424.
Yu W, Wu Y, Yang G. 2014. Early diversification trend and Asian origin for extent bat lineages. *Journal of Evolutionary Biology*, **27**(10): 2204−2218.
Zsebők S, Son NT, Csorba G. 2014. Acoustic characteristics of the echolocation call of the disc-footed bat, *Eudiscopus denticulus* (Osgood, 1932) (Chiroptera, Vespertilionidae). *Acta Acustica United with Acustica*, **100**(4): 767−771.